

A Spatial Filter for Enhanced Detection of Intracranial Sensory Gating Effects

Mark E Pflieger¹, Oleg Korzyukov², Richard E Greenblatt¹, Timm Rosburg³, Nash N Boutros²



¹Source Signal Imaging, Inc., San Diego, USA

²Wayne State University, Detroit, USA

³University of Bonn, Bonn, Germany



Presented May 19, 2007 at Society of Biological Psychiatry, San Diego.

Online at http://www.sourcesignal.com/SOBP_2007_Poster.pdf

Abstract in: *Biological Psychiatry* 61(8S):204S

Correspondence: Mark E Pflieger
Source Signal Imaging, Inc.
2323 Broadway, Suite 102
email: mep@sourcesignal.com
phone: 619-234-9935
<http://www.sourcesignal.com>

Objectives of this study were two-fold:

- [1. Scientific content]
 - To identify—using human intracranial EEG data—brain regions and early (<190 ms) latency intervals that are involved in auditory habituation (*sensory gating*) and sensitization.
- [2. Analysis methodology]
 - To apply suitable statistical tests *within subjects*; then to pool statistical results across subjects, regions, and intervals.
 - To determine if a particular *spatial filter* may enhance statistical detection.

Background

Sensory gating dysfunction, assessed via paired-click (S1, S2) extracranial EEG/MEG measures (e.g., impaired habituation of the P50 response), is a useful endophenotype for schizophrenia and bipolar disorder (Cadenhead et al., 2002; Louchart-de la Chapelle et al., 2005; Ahveninen et al., 2007). Intracranial EEG (iEEG) from consenting epilepsy patients provides a unique opportunity to study the complex and poorly understood brain network that supports sensory gating function in humans. A first publication of intracranial sensory gating effects (Grunwald et al., 2003) reported that only a few neocortical areas (most notably: temporal-parietal and prefrontal areas) showed early (~50 ms) sensory gating effects; and that hippocampal gating could be detected only within a later (~250 ms) time window. More detailed examination of medial temporal lobe structures (Boutros et al., 2005) revealed gating of hippocampal (starting ~190 ms) and rhinal (starting ~240 ms) components with opposite polarity. The authors hypothesized earlier (neocortical) and later (medial temporal) stages of gating.

An in-progress study of functional connectivity in the sensory gating network (Pflieger et al., 2006) led us to re-examine some iEEG datasets statistically *within individual subjects using single trial data*; and we applied a phase-locked signal-to-noise ratio (PLSNR) spatial filter in order to improve single trial SNRs of gated components. We asked in the present study: *Does PLSNR filtering improve statistical power so that intracranial gating effects may be detected more extensively or earlier than reported previously?* To address this question, we applied a S1-S2 paired permutation test and contrasted statistical detection results obtained using filtered versus unfiltered gating-related responses.

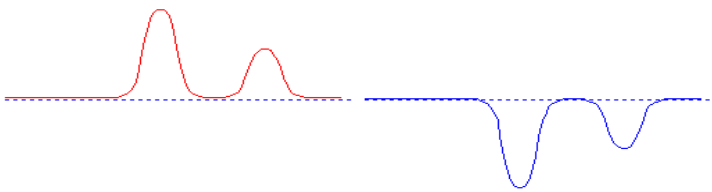
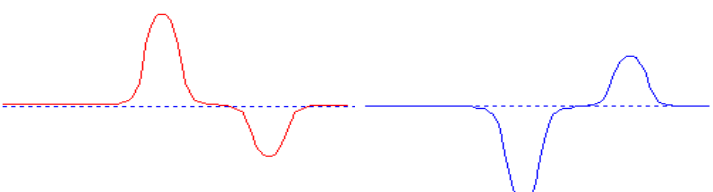
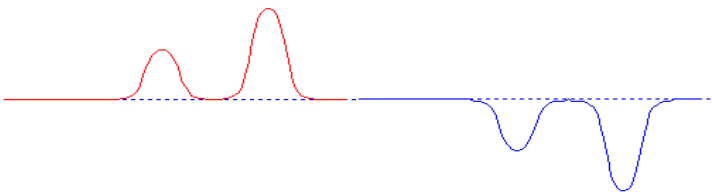
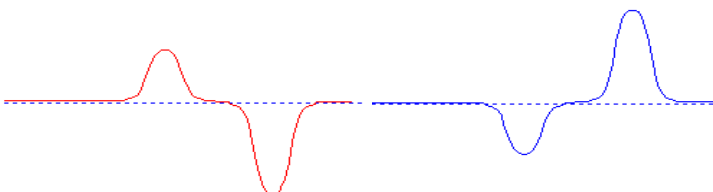
| Four logical possibilities if $S1 \neq S2$ | | |
|--|--|--|
| | Not Opposite Polarity | Opposite Polarity |
| $ S1 > S2 $ |  <p><i>Habituation (Gating)</i></p> |  <p><i>Contrapolar Habituation</i></p> |
| $ S1 < S2 $ |  <p><i>Sensitization</i></p> |  <p><i>Contrapolar Sensitization</i></p> |

Figure 1. Illustrated are four possibilities on the condition that the amplitudes of S1 and S2 are unequal. *Habituation* or *gating* implies that the amplitude of S2 is less than that of S1, and that there is no change in polarity; whereas the polarities of S1 and S2 are opposed in “*contrapolar habituation*”. Likewise, *sensitization* implies that the amplitude of S2 is greater than that of S1, and that there is no change in polarity; whereas the polarities opposed in “*contrapolar sensitization*”. Note that (as defined here) the amplitude of S2 may be zero in habituation, and the amplitude of S1 may be zero in sensitization.

Theory

Within-Subject Statistics Using Single Trial Data. Within-subject p-values for habituation, sensitization, and their contrapolar variants may be obtained using a nonparametric permutation test for S1-S2 paired comparisons (Greenblatt & Pflieger, 2004). The distribution for the null hypothesis ($S1=S2$) is obtained by randomly swapping the roles of S1 and S2 on single trials. Due to many iEEG channels and latencies in a time window of interest, it is necessary to correct for multiple comparisons using the distribution of extreme values across all channels and latencies. Finally, group results may be obtained by pooling statistically significant results across subjects, channel categories (representing brain regions), and latency intervals.

Phase-Locked Signal-to-Noise Ratio (PLSNR) Filtering. A PLSNR filter projects the multichannel data to a subspace of spatial components having $SNR > 1.0$. As illustrated in Figure 3, a PLSNR filter enhances components that are phase-locked to the time of stimulus presentation by discarding those components that are *not* phase-locked to the stimulus presentation. The filter is a matrix that is obtained by estimating certain cross-channel statistics in a latency window of interest. For mathematical details, see the **Appendix**.

Methods

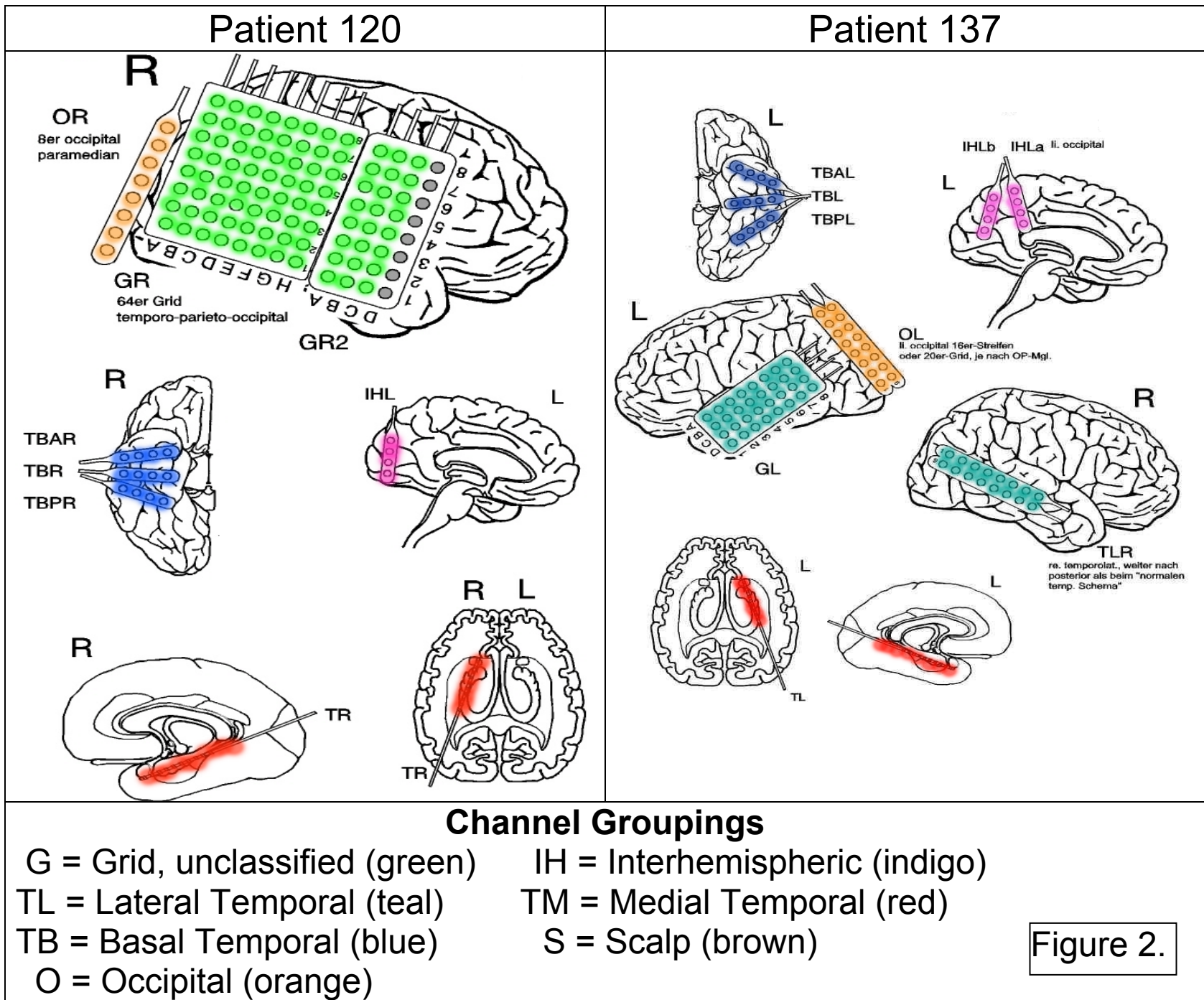
Subjects. Experimental procedures were institutionally approved, and all subjects gave informed consent. Data were analyzed from *eleven epilepsy patients* with simultaneous depth (medial temporal), brain surface, and scalp surface electrodes.

Paradigm. 100 pairs of clicks (first click = S1, second click = S2; 1500 Hz, 4 ms duration, 1.2 ms Gaussian envelope onset and decay) were presented with an inter-click interval of 500 ms and an inter-pair interval of 8 s (Zouridakis & Boutros, 1992). In a sound-shielded room, the patient was instructed merely to listen to the stimuli.

Data acquisition. Surgical implantation utilized grid, strip, and depth electrodes, including (typically) five simultaneous scalp channels. All channels were referenced to linked ears and digitized at 1000 Hz, with bandpass filters at 0.03 – 85 Hz.

Data post-processing. The data were highpass filtered above 4 Hz to insure adequate return to baseline after S1 and before S2. An iterative, automatic outlier rejection algorithm was applied to the continuous data; on average, about 15 out of 100 trials were rejected. A PLSNR filter was trained to 30-190 ms post-stimulus (for both S1 and S2); subsequently, either it was turned off or on.

Statistical analysis. As described above, nonparametric S1-S2 permutation tests were performed per subject. Statistical results were pooled across subjects using three time intervals of interest (30-82 ms, 83-136 ms, 137-190 ms) and seven channel groupings as illustrated in Figure 2. (Note that these channel groupings are a relatively crude first approximation; we plan to reanalyze using more refined groupings.) Results are presented in Figures 4-7.



Unfiltered vs. PLSNR Filtered Paired-Click Averages

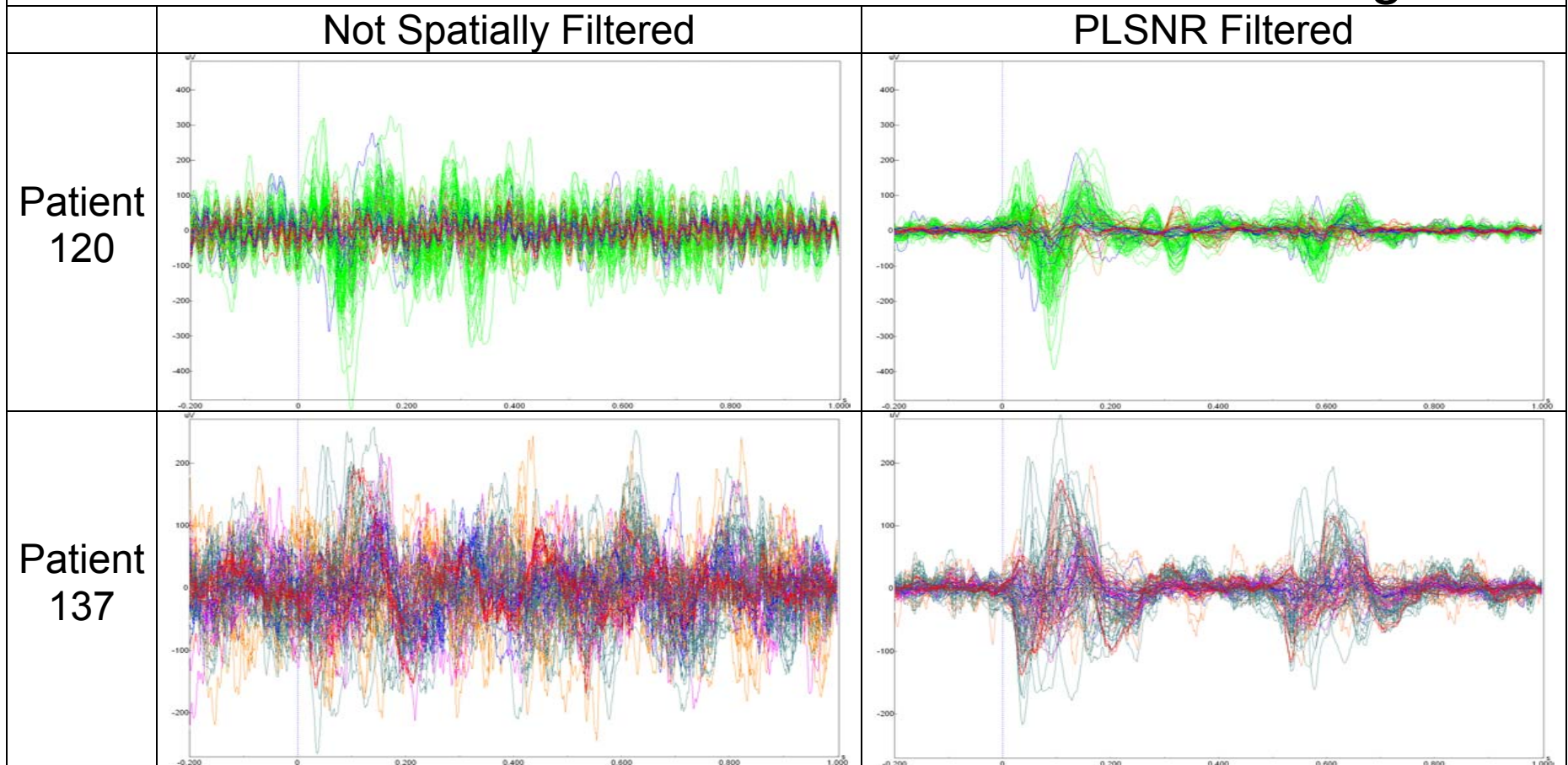


Figure 3. Butterfly plots (all channels superimposed) are presented for averages from two subjects. Trace colors correspond to the electrode colors of Figure 2. For patient 120, notice that the filter eliminated 50 Hz noise (which was not phase-locked to the stimulus). For patient 137, other large non-phase-locked activity was markedly reduced. The prestimulus baseline improved in both cases, and components were enhanced after both S1 and S2 in the time range of interest, namely, 30-190 ms. For statistical purposes, the PLSNR filter was applied to the single trial data.

Statistical Detection of **Habituation** Responses

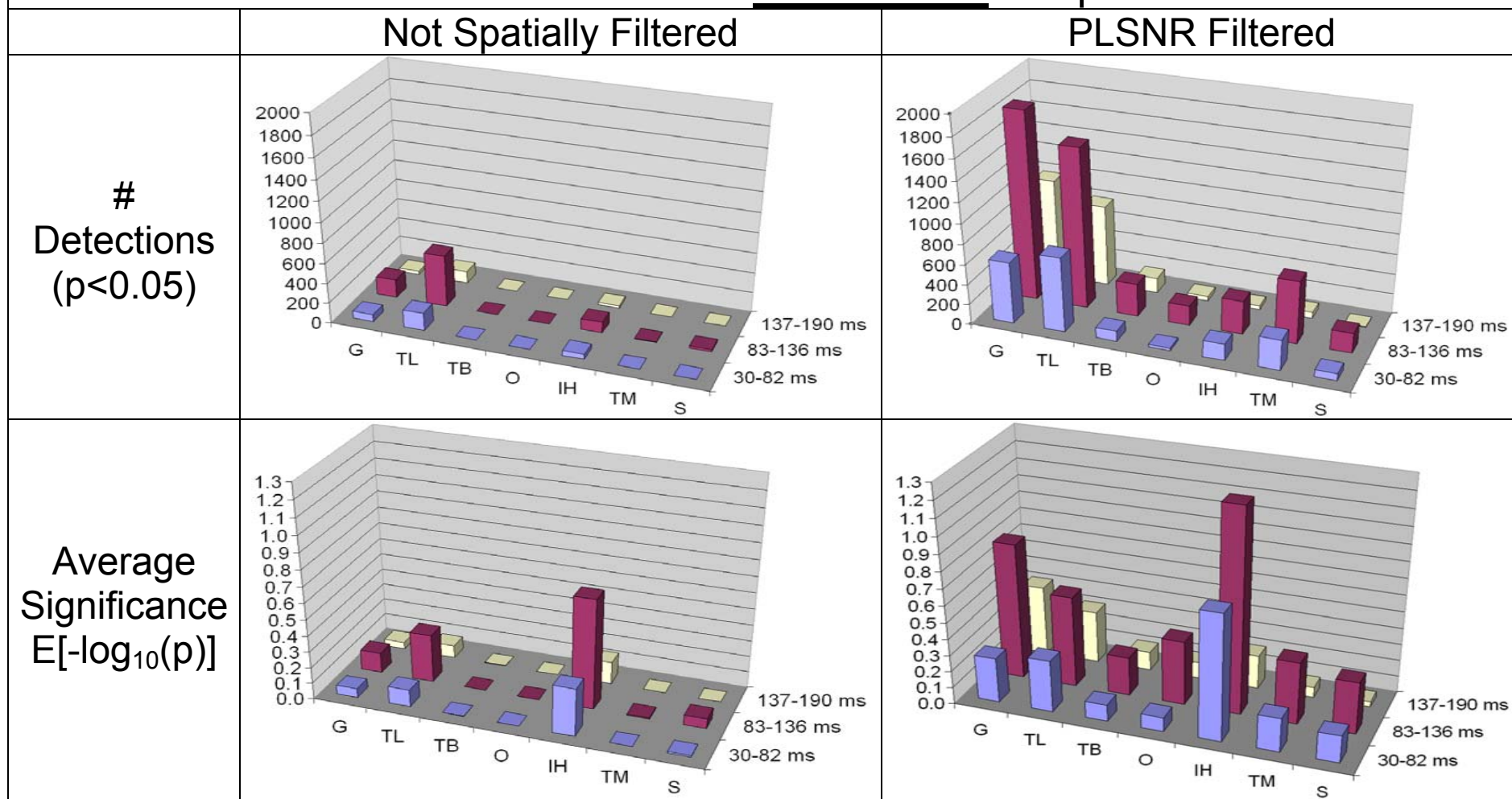


Figure 4. Number of statistical detections ($p < 0.05$, corrected) for habituation responses, and average significances, are compared for unfiltered and filtered data. The seven channel groupings appear in the left-right axis, and the three latency windows in the front-back axis. PLSNR filter yields many more detections, and greatly increased average significance. Larger average significance values for IH channels indicate that these, though fewer in total number, are more consistently prone to habituate.

Statistical Detection of **Contrapolar Habituation** Responses

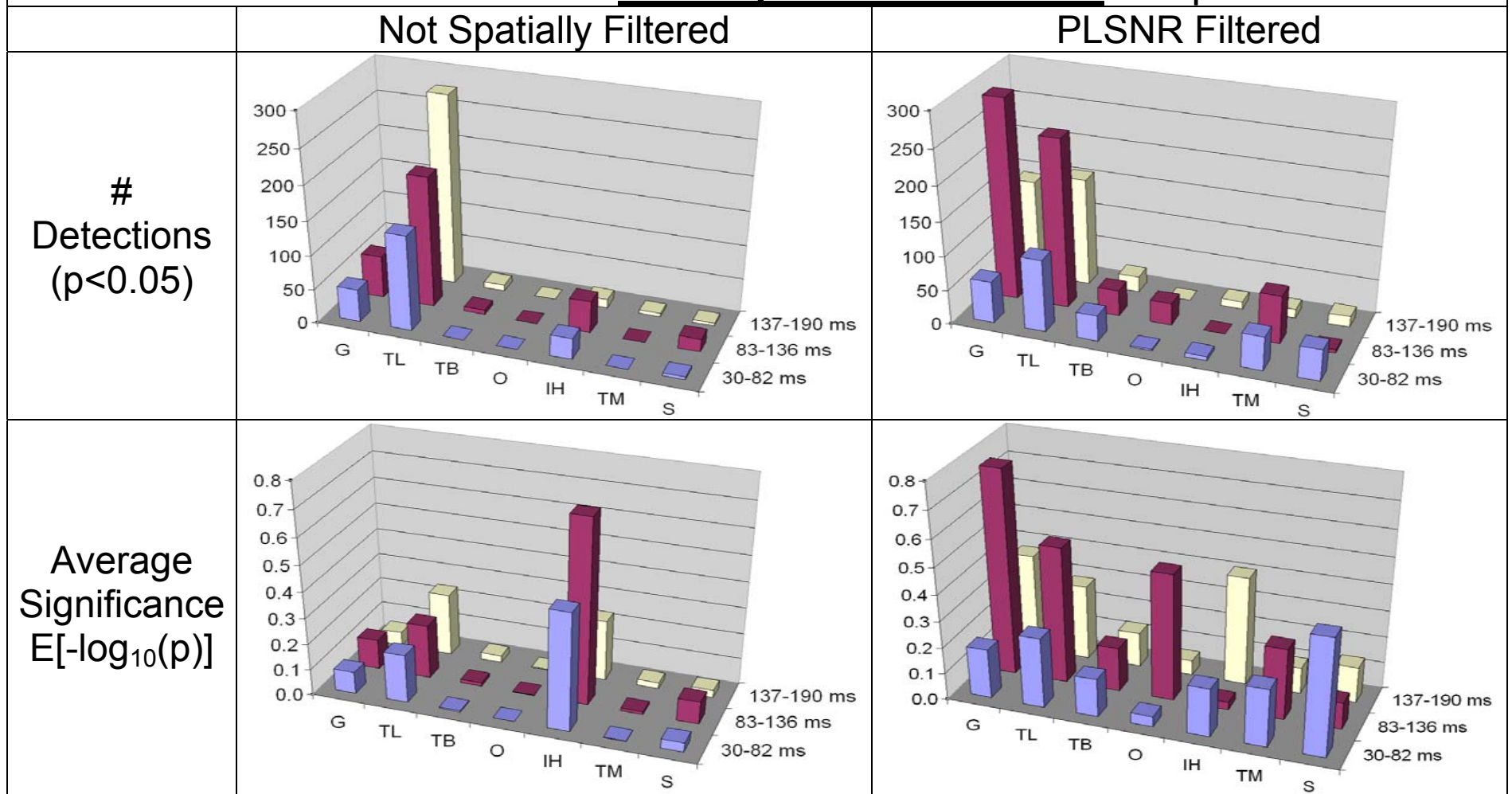


Figure 5. Results for contrapolar habituation. Note the change of scales compared with Figure 4. Overall, the PLSNR filter performs better than for unfiltered data; however, we see occasional examples when the unfiltered case has more detections (TL region, 137-190 ms) and higher average significance (IH, 30-136 ms).

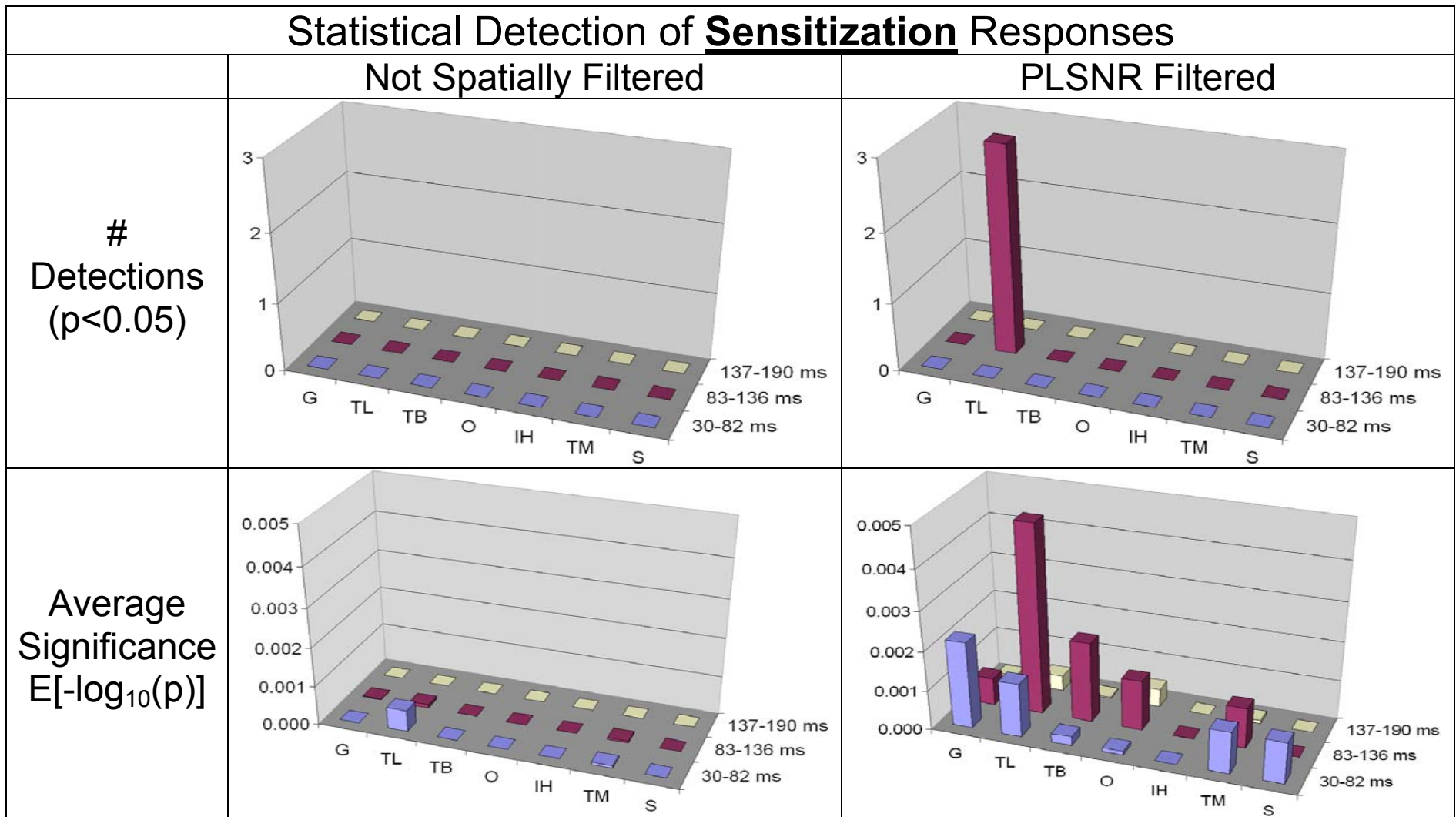


Figure 6. Results for sensitization are striking for the absence of detections: Zero for unfiltered data, and only 3 for filtered data. Average significances are practically negligible (note the scale). Inspection of filtered data detections revealed S1 amplitudes near zero. Thus, sensitization effects are essentially null for these data.

Statistical Detection of **Contrapolar Sensitization** Responses

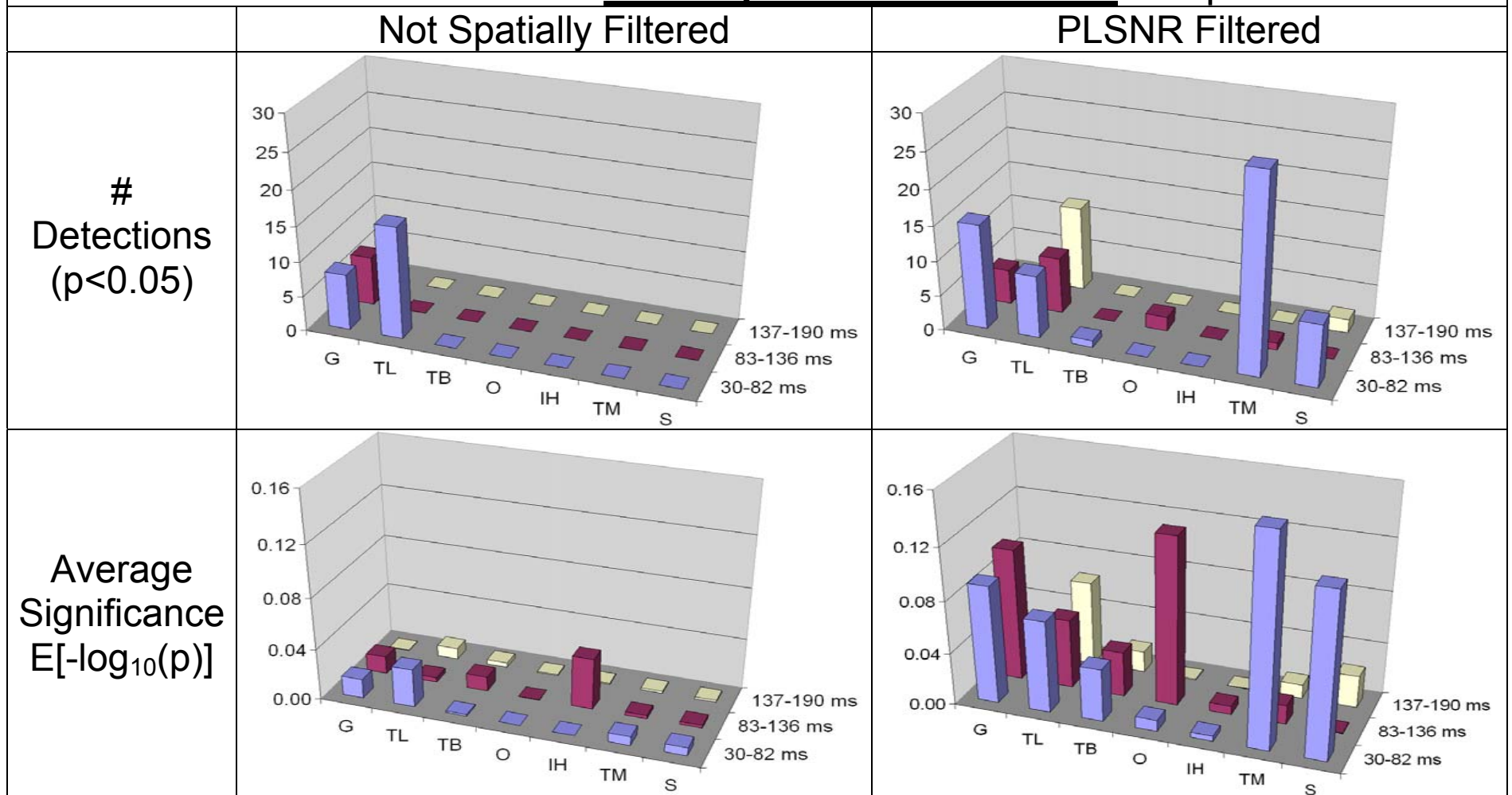


Figure 7. Contrapolar sensitization, although rare, is found most frequently early (30-82 ms) in medial temporal structures.

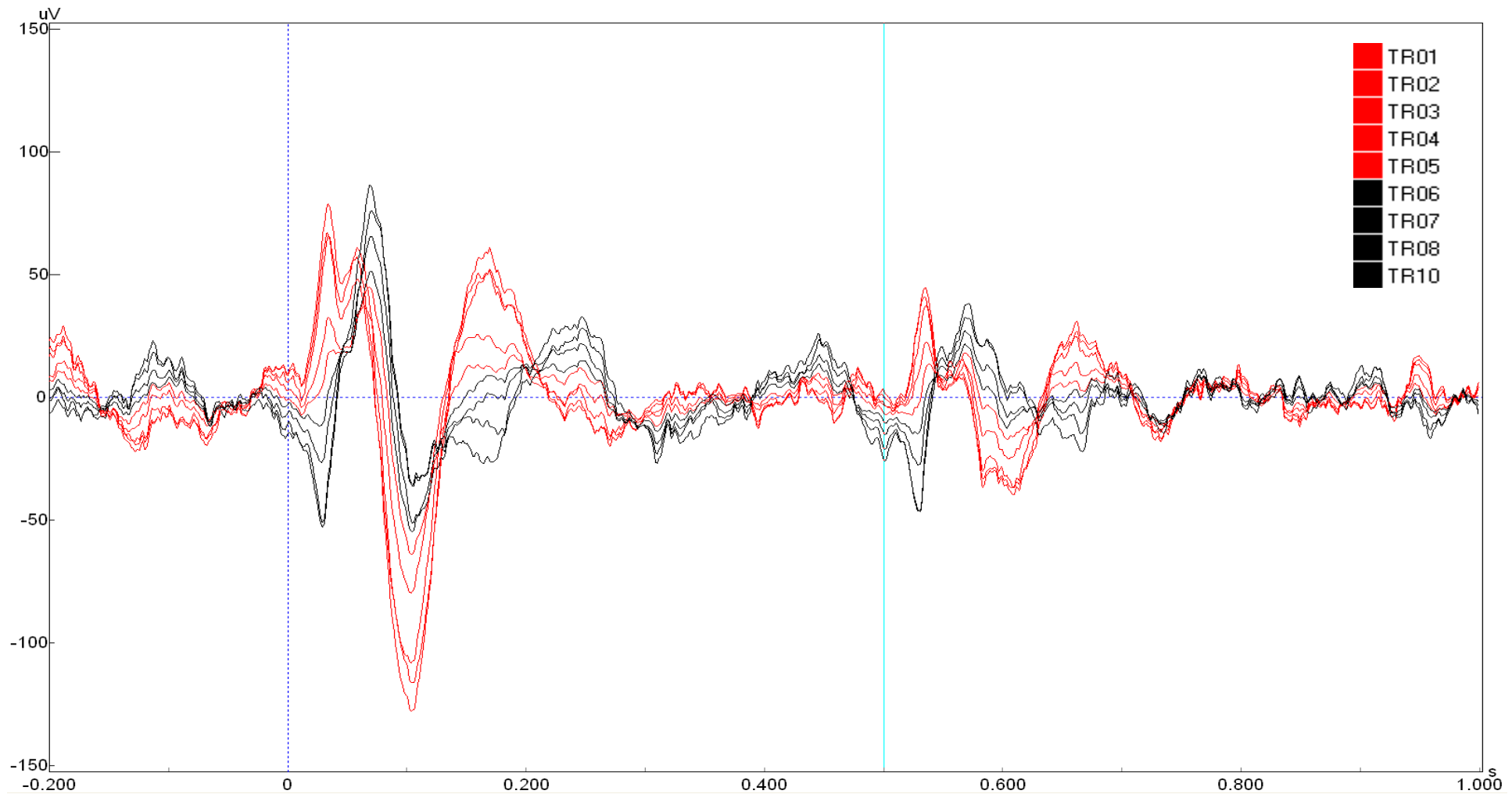


Figure 8. Patient 115 PLSNR filtered averages for medial temporal depth electrodes show highly significant early gating effects. Earliest responses are posterior (likely hippocampal; see black traces) in the 30 ms range, followed a few ms later by polar opposite responses in anterior leads (likely rhinal; see red traces). Before 100 ms, both red and black traces have the same polarity, and appear relatively synchronized. Reduced responses of similar morphology are seen following S2. Note the extreme gating of the 100 ms component.

Conclusions

- Phase-locked SNR filtering enabled the detection of many more sensory gating responses than could be detected without filtering.
 - Single-trial noise variance reduced.
- In particular:
 - Gating regions not previously discussed were identified (e.g., IH).
 - Early (30-100 ms) gating responses were found in hippocampal formation structures.

References

- Ahveninen J, Jääskeläinen IP, and ten others. Inherited auditory-cortical dysfunction in twin pairs discordant for schizophrenia. *Biol Psychiatry* 2007; 60: 612-20.
- Boutros NN, Trautner P, Rosburg T, Korzyukov O, Trunwald T, Cshaller C, Elger CE, Kurthen M. Sensory gating in the human hippocampal and rhinal regions. *Clin Neurophysiol* 2005; 116: 1967-74.
- Cadenhead KS, Light GA, Geyer MA, McDowell JE, Braff DL. Neurobiological measures of schizotypal personality disorder: defining an inhibitory endophenotype? *Am J Psychiatry* 2002; 159: 869-71.
- Greenblatt RE, Pflieger ME. Randomization-based hypothesis testing from event-related data. *Brain Topogr* 2004; 16(4): 225-32.
- Grunwald T, Boutros NN, et al. Neuronal substrates of sensory gating within the human brain. *Biol Psychiatry* 2003; 53: 511-9.
- Louchart-de la Chapelle S, Nkam I, and twelve others. A concordance study of three electrophysiological measures in schizophrenia. *Am J Psychiatry* 2005; 162: 466-74.
- Nichols TE, Holmes AP. Nonparametric permutation tests for functional neuroimaging: A primer with examples. *Human Brain Mapp* 2002; 15(1): 1-25.
- Pflieger ME. Probable bilateral anti-synchronous dynamics for lower quadrant visual field evoked responses. *Intl Congress Series* 1998; 1147: 239-44.
- Pflieger ME, Halgren E. Complementary MEG/EEG information increases with the number of combined experimental conditions. T. Yoshimoto et al. (Eds), *Recent Advances in Biomagnetism*, Tohoku University Press 1999; pp. 294-7.
- Pflieger ME, Korzyukov O, Boutros NN. Coupling and timing of lateral prefrontal cortex and hippocampus during auditory sensory gating: A preliminary analysis of human intracranial EEG data. Online at http://www.sourcesignal.com/SAND3_2006_Causality_Poster.pdf.
- Pflieger ME, Nakada T. The spatial resolving power of high-density EEG: An assessment of limits. T. Nakada (Ed), *Integrated Human Brain Science*, Elsevier Science 2000; pp. 147-91.
- Zouridakis G, Boutros NN. Stimulus parameter effects on the P50 evoked response. *Biol Psychiatry* 1992; 32:839-41.

Acknowledgments: Supported by NIBIB EB000614 (MEP) and NIMH MH063476 (NNB). Thanks to Mary Pflieger for valuable assistance with data analysis.

Appendix

Phase-Locked SNR Filter: Mathematical Details

Following Pflieger (1998), Pflieger & Halgren (1999), and Pflieger & Nakada (2000), we assume a phase-locked signal plus non-phase-locked noise model of the data

$$\mathbf{d}_i(t) = \mathbf{f}(t) + \mathbf{b}_i(t)$$

where $\mathbf{d}_i(t)$ is an M -channel vector for raw data epoch i at time t ; $\mathbf{f}(t)$ is the channel vector for the foreground (phase-locked) brain signal at time t ; and $\mathbf{b}_i(t)$ is a channel vector for a background (non-phase-locked) brain signal for epoch i at time t , which is assumed to be generated by a zero-mean, stationary, multivariate Gaussian process. The crossproduct of sums and the sum of crossproducts matrices are defined as

$$\mathbf{CP}_{\text{sum}} \equiv \sum_{t=1}^T \left(\sum_{i=1}^I \mathbf{d}_i(t) \right) \left(\sum_{i=1}^I \mathbf{d}_i(t) \right)^T, \quad \mathbf{SUM}_{\text{cp}} \equiv \sum_{i=1}^I \sum_{t=1}^T \mathbf{d}_i(t) \mathbf{d}_i(t)^T$$

where I is the number of epochs included in the condition(s) and T is the number of points in the interval of interest. Unbiased estimates of the foreground crossproducts and background covariance matrices are

$$\mathbf{CP}_f \cong (\mathbf{CP}_{\text{sum}} - \mathbf{SUM}_{\text{cp}}) / TI(I - 1)$$

$$\mathbf{COV}_b \cong (\mathbf{SUM}_{\text{cp}} - \mathbf{CP}_{\text{sum}} / I) / TI(I - 1)$$

where the background covariance has been scaled as a residual after averaging over I epochs. Define the SNR matrix, and its singular value decomposition, as

$$\mathbf{SNR} \equiv \mathbf{COV}_b^{-1/2} \mathbf{CP}_f \mathbf{COV}_b^{-1/2}$$

$$\text{svd}(\mathbf{SNR}) = \mathbf{U} \mathbf{W} \mathbf{U}^T$$

The singular values may be interpreted as signal-to-noise ratios, and have the special property of decreasing to a plateau at SNR=1.0. Thus, the PLSNR filter retains only those components with SNR>1.0.

Let r be the number of retained components, and let \mathbf{U}_r be the restriction of \mathbf{U} to r columns. Then the PLSNR filter matrix (in data space) is:

$$\mathbf{F}_{\text{data}} = \mathbf{COV}_b^{+1/2} \mathbf{U}_r \mathbf{U}_r^T \mathbf{COV}_b^{-1/2}.$$